Journal of Applied Electrochemistry **32**: 709–715, 2002.

Influence of copper anion complexes on the incorporation of metal particles in polyaniline
Part II: Copper oxalate complex

S. IVANOV and V. TSAKOVA*
Institute of Physical Chemistry, Bulgarian Academy of Sciences, Bg-1113 Sofia, Bulgaria
*(*author for correspondence, fax: +359 2 9712688, e-mail: tsakova@ipchp.ipc.bas.bg)*

Received 11 December 2001; accepted in revised form 27 March 2002

Key words: copper electrodeposition, microcrystals, oxalate metal complexes, polyaniline

Abstract

Copper deposition at polyaniline (PAN) coated electrodes is studied using copper oxalate complexes as reducing species. It is found that a high number (3.4×10^8 cm^{-2}) of single sized (~150 nm), regular shaped crystals can be obtained. Statistical analysis of the distances between neighbouring crystals shows deviation from a random surface distribution. This finding is discussed both in terms of origin and overlap of nucleation exclusion zones and of the influence of the finite size of the copper crystals. Experiments performed under potentiostatic conditions give evidence for instantaneous copper nucleation and growth under phase boundary transition limitations. Results concerning number, size and shape of copper crystals deposited in a similar way using three different reducing species (i.e., copper cations, copper citrate and copper oxalate complex anions) are compared. It is established that the copper oxalate complex anions allow for deposition of the largest number of small metal crystals. This result is related to both the initial oxidation state of the PAN layer in the oxalate solution and to the specific properties of the anion complex.

1. Introduction

Although of common use in metal plating, metal ion complexes have not so far been studied with respect to their effect on metal electrodeposition in conducting polymer layers. Anion complexes of noble metals were often used as the only available source for metal reduction (e.g., [1–13]). In some cases [l, 2, 6–8] Pt, Pd and Rh complex anions have been employed with the special intention of binding the anionic species to the partial positive charge of the polymer chains and making effective the next step of metal reduction in the bulk of the polymer layer. In all these investigations there was no possibility for comparing the electrodeposition using cataionic and complex anionic species of one and the same metal and thus for clarifying the specific role of the anionic complexes. However, this could be easily done with other metals (e.g., copper or silver), offering the possibility to use both the non-complexed metal cation and a large variety of complex metal ions. To our knowledge, little use of this strategy has been made so far.

Copper electrodeposition in functionalized polypyrrole using a copper oxalate solution was studied by Zouaoui et al. [14]. The exchange of the anionic species bound at the polymer chains with copper oxalate anions was carried out in a preliminary step and was followed by electroreduction of the copper anionic species. It was found that the deposited metal particles range from 50–100 up to 300 nm and are formed by initial nucleation at the polymer/underlying carbon interface and further growth through the polypyrrole film [14]. However, in this case, too, no direct comparison was performed with the deposition of copper in the same polymer layers using copper cations as reducing species.

In the first part of our study [15] we explored the influence of the copper citrate anions on the copper deposition in polyaniline (PAN). The results were compared to previous investigation on copper deposition from a copper sulfate solution [16]. It was found that making use of copper citrate anions allows shifting of the metal deposition potential window and resolving metal and polymer reduction. A strong inhibition of the electrodeposition was also observed and only a small amount of copper could be incorporated in the polyaniline layers. Different effects were suggested as possible reasons for the results [15]. To outline further the specific role of anionic complexes for metal electrodeposition in conducting polymer layers, copper oxalate anions are used as reducing species for the copper

plating process in the present study. Copper oxalate anions have different stability and size in comparison to the copper citrate complex anions used previously.

2. Experimental details

Details of the experimental set-up and equipment were described in the first part of this study. The only difference concerns the solution used for copper deposition. In the present study an aqueous solution of 0.02 M $CuSO_4$, 0.06 M $Na_2C_2O_4$ and 0.344 M K_2SO_4 at pH 6.5 was employed. As in the case of Zouaoui et al. [14], at this pH value and solution composition the oxalate complex $[Cu(C_2O_4)_2]^{2-}$ (denoted further as $CuOx_2$) is the dominating species. According to [17], the stability constant of the $CuOx_2$ complex is $\log K_2 = 9.21$ and is thus definitely higher than the stability constant of the copper citrate complex ($\log K_1 = 5.9$) used in the first part of this study. Besides, from a structural point of view $CuOx_2$ builds a dioxalatecuprate ion [18] (Structure 1) which should be larger then the copper citrate aqua complex.

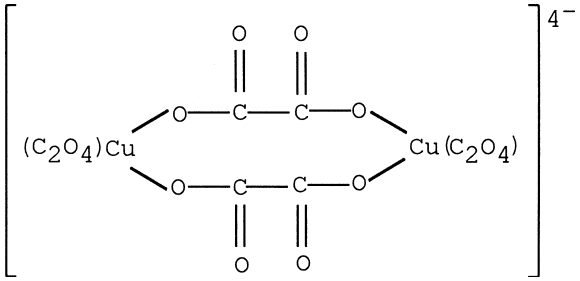

Structure 1.

The equilibrium potential of copper in the copper oxalate solution was measured to be $E_0^{(Cu/CuOx_2)} = -0.547$ V vs MSE and is thus close to the equilibrium potential of the Cu/Cu-citrate couple.

All experiments were performed at PAN layers with one and the same reduction charge, $Q_{red}^{PAN} = 20\,mC\,cm^{-2}$.

3. Results and discussion

3.1. *Potentiodynamic and galvanostatic experiments*

Figure 1 shows potentiodynamic curves (first scans) measured at oxidized PAN coated electrodes in supporting electrolytes (K_2SO_4 + $Na_2C_2O_4$ and K_2SO_4 alone) and in the copper oxalate solution. In the presence of oxalate anions the reduction wave of the PAN layers is slightly shifted in the negative direction compared to the K_2SO_4 solution alone. Thus, in contrast to the citrate anions which make reduction easier (Figure l, Part I), oxalate anions inhibit this process. As a consequence, copper and PAN reduction potential windows overlap to a certain extent in the copper oxalate solution (compare full and dashed lines in Figure 1). This situation seems to be closer to deposition from acid copper sulfate than to that from copper citrate solution. To explore further the exact potential window for copper deposition, galvanostatic reduction was performed at both oxidised and initially reduced (in acid solution) PAN coated electrodes (Figure 2). It is evident that copper deposition in this solution also requires high overpotentials. However, in comparison to copper citrate solution, the overpotentials are about 100 mV lower and maxima also giving evidence for a typical nucleation and growth process appear even for thick PAN coatings. Thus, although with higher stability and, presumably, larger size, copper oxalate complexes give a more efficient metal deposition process than copper citrate complexes. This is an unexpected result demonstrating that the characteristics of the complex anions alone are not always of major importance. Other factors, such as exact oxidation state of the polymer layers at the beginning of metal deposition very probably play a significant role in the overall plating process.

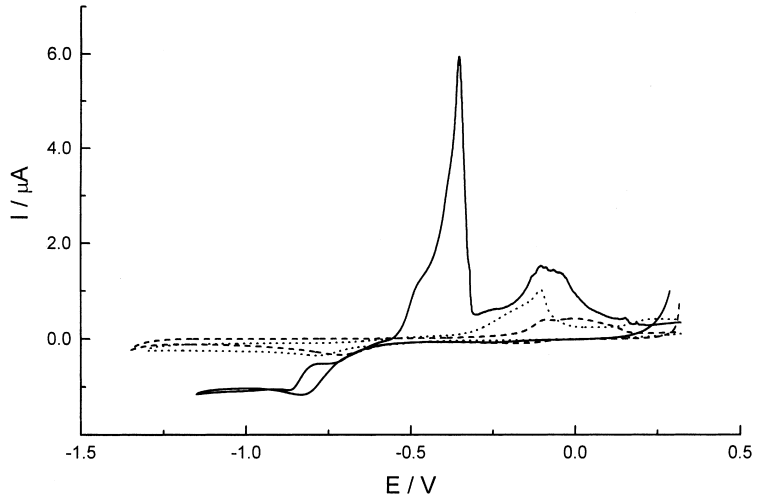

Fig. 1. Potentiodynamic curves measured at a PAN coated electrode in the copper oxalate solution (——), in 0.344 M K_2SO_4 + 0.06 Na_2Ox (···) and in 0.344 M K_2SO_4 (- - -) solutions.

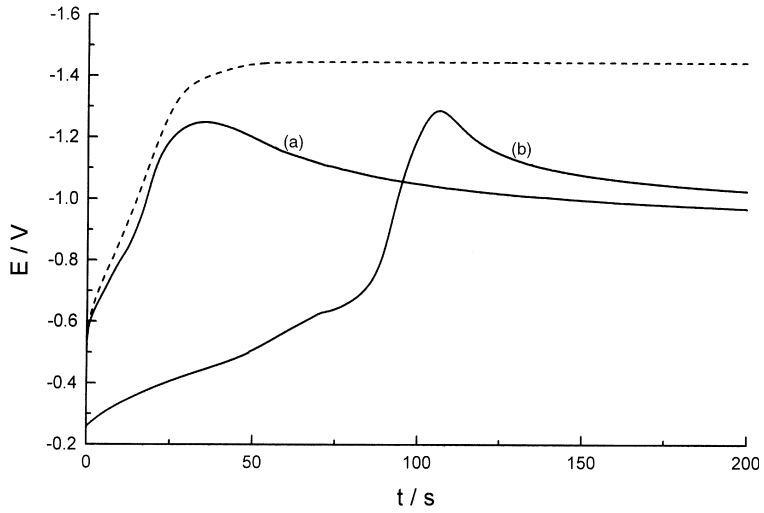

Fig. 2. Galvanostatic copper deposition curves measured at (a) reduced and (b) oxidized PAN coated electrodes. Dashed line denotes galvanostatic curve measured in supporting electrolyte (K_2SO_4 + Na_2Ox) at the reduced PAN layer. (Reduction of the PAN layer occurred in acid 0.5 M H_2SO_4 solution.)

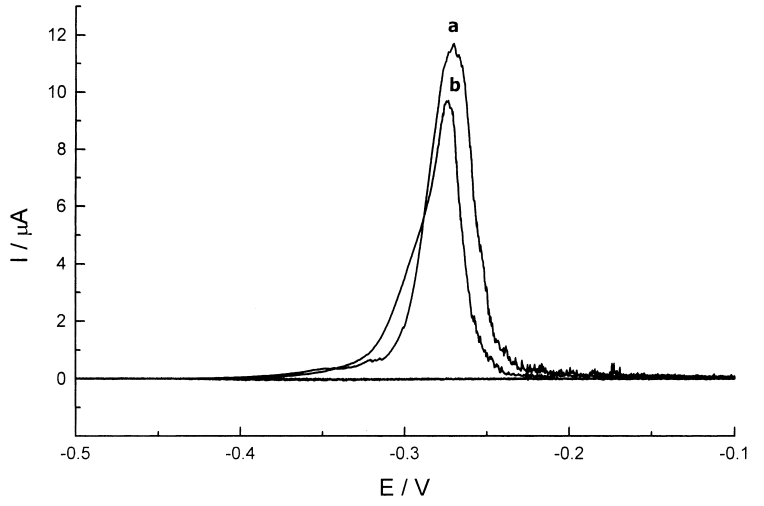

Fig. 3. Copper oxidation curves registered after galvanostatic deposition at the reduced (a) and oxidised (b) PAN coated electrodes.

As in our previous study, after galvanostatic deposition, anodic sweep curves were measured at a slow scan rate (Figure 3). A single well resolved copper oxidation peak (centered at about −0.270 V) was found for both oxidised and initially reduced PAN layers even for large amounts of deposited copper. This peak overlaps with the second, most positive oxidation peak registered in the case of deposition from the copper citrate solution. In contrast to the copper citrate case, with increasing amount of deposited copper this single oxidation peak also grows further and no other (more negative) oxidation peak emerges. Thus, larger amounts of copper may be incorporated into the polymer layer and a single kind of copper species is formed at the PAN coated electrode.

3.2. *SEM observation and statistical analysis of the crystal surface distribution*

Evidence was obtained by SEM observation of Cu/PAN specimens prepared by galvanostatic deposition in the copper oxalate solution (Figure 4). The copper deposit consists of a high number of regularly shaped crystals of approximately equal size (150 nm). Their number density (3.4×10^8 cm^{-2}) is two orders of magnitude higher than that in the citrate case. Statistical analysis of the distances between first and second neighbouring crystals was performed. The data (Figure 5) show a deviation of the experimental hystograms from the Poissonian prediction, the latter being valid for the case of a two-dimensional surface random distribution. Most often such a deviation is discussed in terms of appearance and overlap of the so called nucleation exclusion zones, or zones of reduced overpotential (ZRO) arising around growing crystals [19–23]. It is known that in the course of a progressive nucleation process the nucleation probability diminishes in the close vicinity of existing crystals due to ZRO. Thus, active sites covered by ZRO cannot be used for nucleation and the number of crystals remains smaller than the number of available active sites for metal deposition. Consequently, the

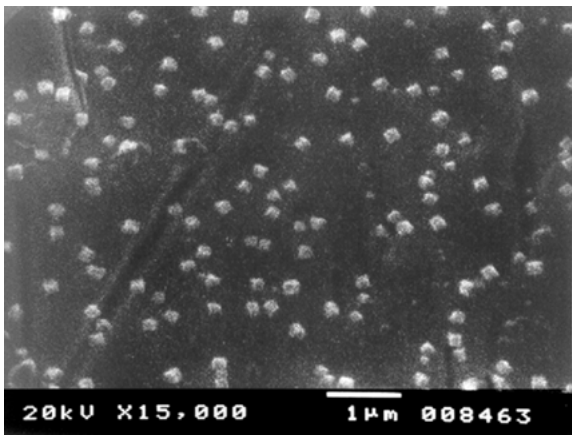

Fig. 4. SEM of copper crystals obtained by galvanostatic deposition at an oxidized PAN layer.

crystal surface distribution deviates from a random distribution. However, if all metal crystals appear simultaneously (i.e., instantaneous nucleation), all active sites should be occupied at once and effects originating from the later stage of crystal growth should not affect the crystal number and surface distribution. Therefore, the deviation from Poissonian behaviour established in these experiments should mean that the nucleation process is progressive and ZRO affects the advanced stage of nucleation. This seems, however, to contradict the experimental observation showing that almost all crystals have the same size (Figure 4), which is evidence for instantaneous nucleation. To clarify this problem the kinetics of the nucleation process was studied by means of potentiostatic current transients.

3.3. *Nucleation kinetics through potentiostatic experiments*

It was found that initiation of copper nucleation and growth occurs at low negative potentials, starting from −0.73 V. Coming back to the galvanostatic deposition curves (Figure 2), this means that, at least for $E < -0.73$ V, current is consumed for both residual reduction of the PAN layer and copper deposition. However, the similarity of shape of both supporting electrolyte and copper containing solution curves indicates that the current up to $E = -1.0$ V is mainly consumed in residual reduction of the polymer layer. Thus, copper

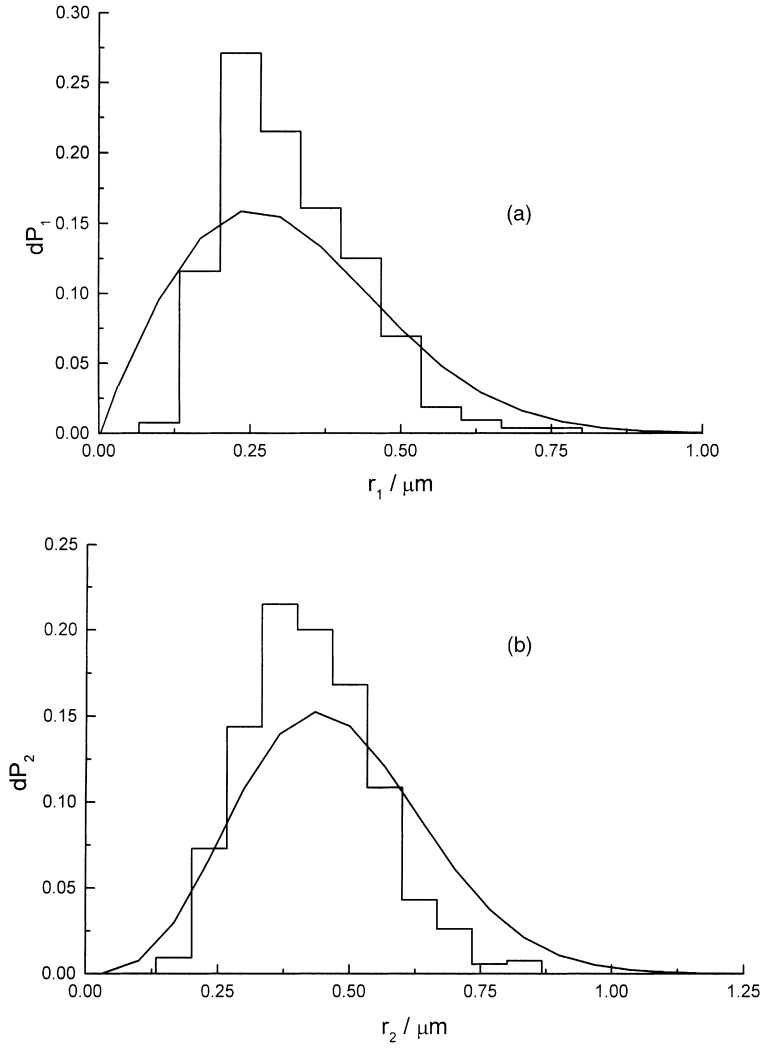

Fig. 5. Experimental (histograms) and Poissonian (full lines) distributions of the distances between first (a) and second (b) neighbouring crystals.

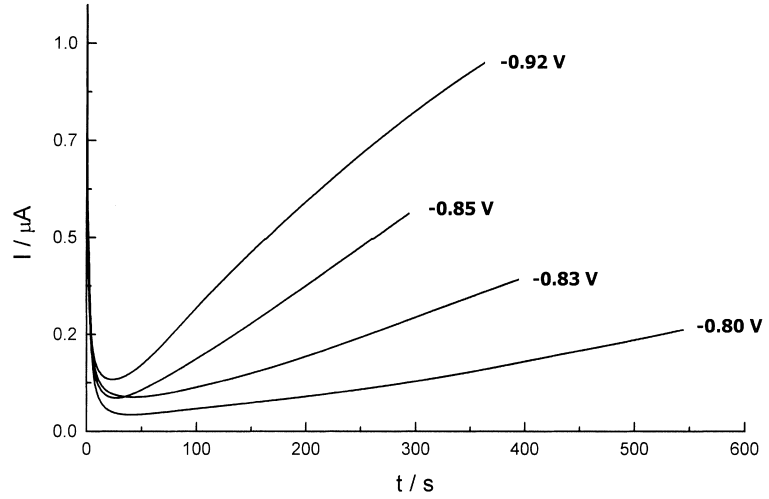

Fig. 6. Potentiostatic current transients of copper deposition obtained at different potentials.

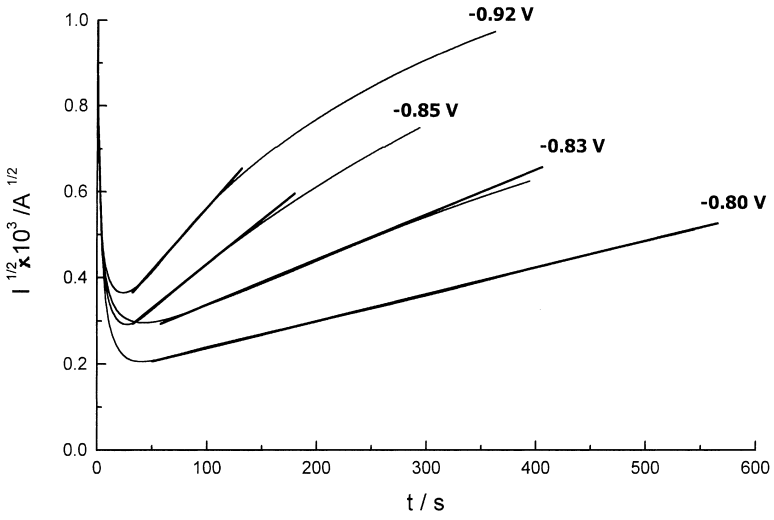

Fig. 7. Linearization of the initial parts of the current transients in Figure 6.

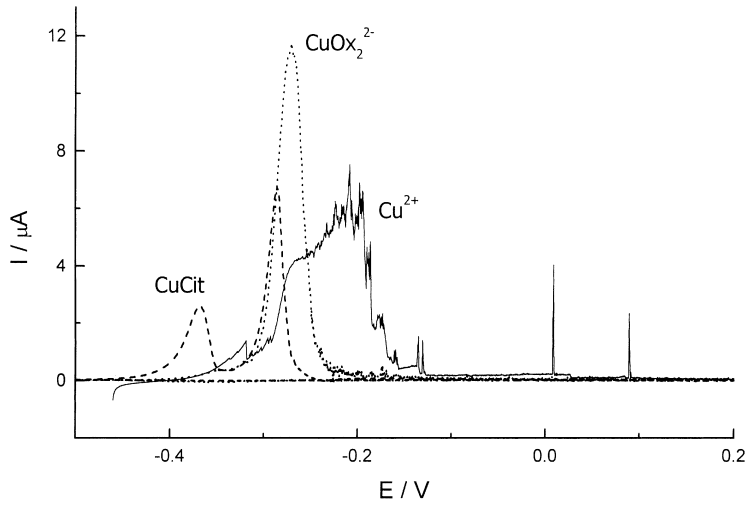

Fig. 8. Copper oxidation after galvanostatic deposition performed with different metal reducing species: (——) Cu^{2+}, (- - -) CuCit and $CuOx_2$ (···).

crystals appear at low overpotentials. Their growth is slow and accompanied by a parallel change in the oxidation state of the polymer layer.

Figure 6 shows a set of potentiostaic current transients taken at different potentials at PAN coated electrodes at the same Q_{red}^{PAN}. Obtaining reproducible results in these

experiments was a tedious task, most probably due to the difficulties in reproducing the polymer structure in each experiment and fixing the same initial oxidation state of the PAN layer. Better results were obtained by using a two step reduction procedure consisting of initial reduction at −0.66 V in the acid solution (0.5 M H_2SO_4) followed by further reduction at −0.55 V in the copper oxalate solution. The next step was to apply a copper deposition pulse. The initial parts of the transients in Figure 6 can be linearized in $I^{1/2}$ against t coordinates (Figure 7). As already discussed in our earlier study [16], such an I/t relationship corresponds to the case of instantaneous nucleation and 3D growth of crystals under phase boundary transition limitations.

The results obtained so far from the potentiostatic study of copper deposition in PAN agree with the microscopic observation giving evidence for instantaneous nucleation of copper crystals in PAN. Therefore, the observed deviation of the surface distribution of copper crystals from a random one cannot be attributed to the effect of ZRO. There are two further possible reasons for such a deviation: first, Poisson distributions are strictly valid for point-like objects with zero dimension and, second, the active sites for nucleation could have a non-random distribution. To assume a more or less ordered distribution of active sites in a non-ordered, amorphous polymer layer seems to be unrealistic. The first reason, mentioned above could, however, apply to explain our results. Indeed, the mean distance between the first neighbouring crystals (315 nm) is only twice as large as the average size of the crystals ($d_{ave} = 150$ nm). It is obvious that distances smaller then d_{ave} will be missing in the distribution (Figure 5). Thus, the finite size of the crystal, which is comparable with the mean distance between neighbouring crystals, is the probable reason for the discrepancy with the Poisson distribution law observed.

3.4. *Comparison of copper deposition from acid copper sulfate, copper citrate and copper oxalate solutions*

The use of the three different copper containing solutions allows copper deposits differing highly in number density, size, location and morphology to be obtained. This can be easily assessed by means of the copper oxidation curves (obtained after galvanostatic deposition of equal quantities of copper in the three solutions studied, Figure 8) and corresponding scanning electron micrographs (Figure 9). As can be seen in Figure 8, only in the case of copper citrate does a more negative copper dissolution peak arise; this is attributable to the presence of large hemispherical, highly defective crystals located on top of the polymer layer. The single well-resolved peak characterising the oxidation of the metal deposit obtained from the oxalate solution corresponds to the

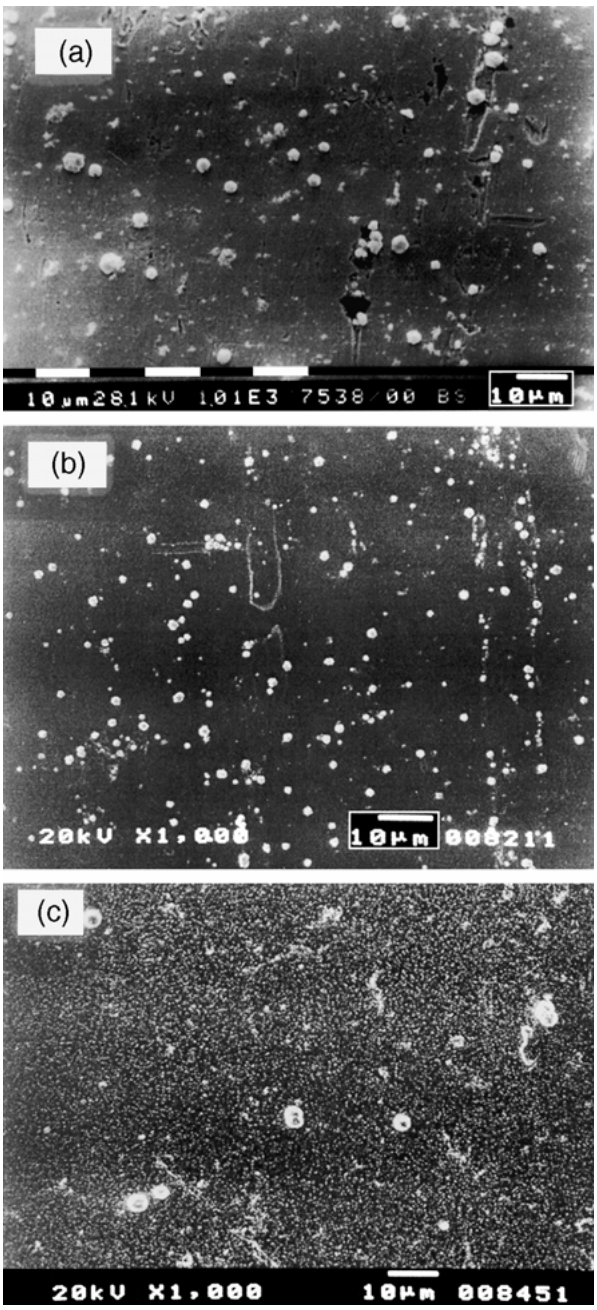

Fig. 9. SEMs of Cu/PAN specimens obtained after galvanostatic deposition by using different reducing species: (a) Cu^{2+}, (b) CuCit and (c) $CuOx_2$.

Table 1. Characteristics of the copper crystals obtained at PAN coated electrodes

Reducing species	Morphology	Mean size /µm	Mean distance /µm	Number of crystals per cm^2
CuCit	spherical crystals	0.3–1.5	2.60	3.6×10^6
$CuOx_2$	regular shaped crystals	0.15	0.31	3.4×10^8
Cu^{2+}	spherical crystals	0.2–2.0	0.47	1.3×10^8

single sized crystals with high number density. As for the usual case of copper sulfate solution, copper is deposited most probably even in the finest porous structure of the PAN layers, which results in a very large positively shifted peak with current spikes at potentials as high as +0.1. V [16]. Looking at the micrographs (Figure 8), it becomes evident that the greatest number of small single sized crystals is obtained in the copper oxalate solution. A summary of the data concerning the number density, average size, mean distance and shape of copper crystals obtained in a similar way in the three solutions is given in Table 1. Obviously, copper deposition from the oxalate solution is best suited for dispersing of a large number of small monosized copper particles.

4. Conclusions

The investigations presented in both parts of this study demonstrate the possibility to influence markedly the metal deposition process in conducting polymer layers by use of metal ion complexes. Copper crystals with different morphology and number densities varying by more than two orders of magnitude could be deposited in/at polyaniline layers depending on the source for metal reduction. Different amounts of copper could also be incorporated in the polymer layer.

The comparison between the two complex copper anions shows that, in the system under consideration, the stability and size of the complex does not play a decisive role. It is rather the interference of two reduction processes: reduction of the polymer layer itself and reduction of the metal ionic species that makes the difference. In fact, the initial oxidation state of the polymer layer is highly dependent on both potential and solution composition (i.e., pH and type of anions). As already shown, in the case of citrate anions, PAN layers undergo reduction before the onset of metal deposition. On the other hand, in the presence of oxalate anions polymer reduction and initial metal deposition go in parallel. It is worth pointing out here that PAN reduction at pH 6.0–6.5 results in the deprotonated, neutral leucoemeraldine state [24] and is very likely accompanied by compression of the polymer structure and expulsion of anions and water molecules. So, the reduced layer should be compact and less permeable for diffusion of large anion complexes. In contrast, the oxidised PAN structure, as obtained in the acid solution, is in the protonated emeraldine state and has positive charges. This allows for an easier transport of anion complexes inside the layer. This is also valid for PAN initially reduced in the acid solution, which retains its positive charge in the protonated leucoemeraldine state. Apart from this important difference, additional peculiarities may arise due to the necessary diffusion of anions released after reduction of the metal complex, out of the polymer layer. This transport should be inhibited for large anions in the compressed PAN structure and be easier for smaller anions in the still partially oxidized PAN layer. Bearing in mind that the single oxalate ion is smaller than the citrate one, this is probably another reason for the easier copper deposition from oxalate complex anions.

Thus, it is evident that the interplay between the oxidation and structural state of the polymer layers and the size and stability of the metal ion complex and its anion constituents should offer a large variety of possibilities for influencing metal deposition in conducting polymer layers.

Acknowledgements

The authors thank Prof. D. Stoychev for fruitful discussions and B. Ranguelov for kind cooperation in obtaining SEM pictures of Cu/PAN specimens. The investigations were completed with the financial support of the Bulgarian Ministry of Science and Education under contract X-1008. The equipment used in all electrochemical experiments was a donation (to V.T.) by the Alexander von Humboldt Foundation, Germany.

References

1. K.M. Kost, D.E. Bartak, B. Kazee and Th. Kuwana, *Anal. Chem.* **60** (1988) 2379.
2. S. Holdcroft and B. Lionel Funt, *J. Electroanal. Chem.* **240** (1988) 89.
3. P. Ocon Esteban, J.M. Leger and C. Lamy, *J. Appl. Electrochem.* **19** (1989) 462.
4. M. Gholamian and A.Q. Contractor, *J. Electroanal. Chem.* **289** (1990) 69.
5. Ch. Hable and M.S. Wrighton, *Langmuir* **9** (1993) 3284.
6. R. Kostecki, M. Ulmann, J. Augustynski, D.J. Strike and M. Koudelka-Hep, *J. Phys. Chem.* **97** (1993) 8113.
7. J-C. Moutet, Y. Ouennoughi, A. Ourari and S. Hamar-Thibault, *Electrochim. Acta* **40** (1995) 1827.
8. M. Hepel, *J. Electrochem. Soc.* **145** (1998) 124.
9. F. Ficicioglu and F. Kadirgan, *J. Electroanal. Chem.* **451** (1998) 95.
10. M.A. del Valle, F.R. Diaz, M.E. Bodini, T. Pizarro, R. Cordova, H. Gomez and R. Schrebler, *J. Appl. Electrochem.* **28** (1998) 943.
11. K. Bouzek, K-M. Mangold and K. Juettner, *Electrochim. Acta* **46** (2000) 661.
12. C. Coutanceau, M. J. Croissant, T. Napporn and C. Lamy, *Electrochim. Acta* **46** (2000) 579.
13. A. Yassar, J. Roncali and F. Garnier, *J. Chem. Phys.* **86** (1989) 241.
14. A. Zouaoui, O. Stephan, M. Carrier and J-C. Moutet, *J. Electroanal. Chem.* **474** (1999), 113.
15. S. Ivanov and V. Tsakova, *J. Appl. Electrochem.*, this issue.
16. V. Tsakova, D. Borissov, B. Ranguelov, Ch. Stromberg and J.W. Schultze, *Electrochim. Acta* **46** (2001) 4213.
17. A.E. Martell and R.M. Smith, 'Critical Stability Constants', Vols 1–3, (Plenum Press, New York, 1977).
18. Gmelin's 'Handbuch der anorganischen Chemie', Vol. 60, Tl.B, Lfg.2, pp. 798–799.
19. A. Milchev, E. Vassileva and V. Kertov, *J. Electroanal. Chem.* **107** (1980) 323.
20. A. Milchev, *Electrochim. Acta* **28** (1983) 947.
21. A. Serruya, J. Mostany and B.R. Scharifker, *J. Chem. Soc. Faraday Trans.* **89** (1993) 255.
22. W.S. Kruijt, M. Sluyters-Rehbach, J.H. Sluyters and A. Milchev, J. *Electroanal. Chem.* **371** (1994) 13.
23. U. Scmidt, M. Donten and J.G. Osteryoung, *J. Electrochem. Soc.* **144** (1997) 2013.
24. W-S. Huang, B. Humphrey and A.G. Macdiarmid, *J. Chem. Soc., Faraday Trans.* **82** (1986) 2385.